Journal of the National Academy of Forensic Engineers®

http://www.nafe.org

ISSN: 2379-3252

Vol. 38 No. 1 June 2021

Computational Fluid Dynamics Modeling of a Commercial Diving Incident

By Bart Kemper, PE (NAFE 965S) and Linda Cross, PE

Abstract

A commercial diver using surface-supplied air was "jetting" a trench, which was using high-pressure water via an industrial "jetting hose" connected to a pressure-compensated tool to cut trenches in silty sea bottoms. This tool used high-pressure water pumped from the tender boat down to the diver. It was reported that man-made objects in the area cut the jetting hose, resulting in uncontrolled diver movement and subsequent injury. There were no direct witnesses available. The subsequent forensic engineering investigation used traditional calculations, laboratory testing, ergonomics, biomechanics, and computational fluid dynamics (CFDs) to determine the limits of the physics involved in order to assess the feasibility of the reported scenario. Specifically, CFD modeled the mass flow exiting the tool's two ends and the cut in the hose as well as modeled the diver's flow resistance while propelled through the water. The results indicated the applicable physics precluded the events as described.

Keywords

Diving, computational fluid dynamics, CFD, flow resistance, friction loss, jetting, forensic engineering, biomechanics

Introduction

One effective approach in dealing with a forensic case is to examine the chain of events required to go from a safe or neutral state to a damaged state, which is typically the crux of litigation. Sometimes, the chain of events is simple: A distracted driver speeds through an active cross walk, striking and killing a pedestrian in full view of witnesses and multiple cameras. A forensic engineer is unlikely to be called upon unless it is to establish whether a potential defect or condition significantly contributed to the event.

Some cases have no witnesses, no cameras, and no direct data to corroborate or impeach the statements of an injured party. Experimentation can be difficult or impossible due to the on-site conditions or risks associated with the events. In such instances, engineering work can be the key to establishing the conditions needed for each link in the chain to be feasible in order to assess whether the chain of events could link from the issue or state being litigated to a known state or condition[1]. Determining whether the required chain of events is physically feasible can be a decisive tool for ending the litigation. This confirmation of the chain of events also lays the foundation for follow-on work to evaluate a more nuanced scenario of "how did this happen" rather than "did this happen," as appropriate.

Diving Incident

This case study involved a commercial diver using supplied air working from a diving barge. This is different than the diving with air tanks many are more familiar with. The diver's primary air supply is via a hose provided from the surface, connected to a diving helmet encompassing the entire head and allowing the diver to speak to support crew on the surface. The diver typically is walking on the bottom instead of swimming. An example of what this work environment is like is shown in **Figure 1**.

Figure 1
An example of a commercial diver performing work on the bottom of a sea or lake. Cutting trenches using jetting nozzles is done in zero visibility due to the dense clouds of silt the process creates. (Photo credit: Dive Safe International, released for public use)

Bart Kemper, PE, 4520 Jamestown Ave., #3 Baton Rouge, LA 70808, (225) 923-2945, bkemper@kempereng.com
DOI: 10.51501/jotnafe.v38i1.66

Federal occupational safety rules apply to commercial diving[2], which, in turn, (per OSHA Directive Number CPL 02-00-151) incorporate "International Consensus Standards For Commercial Diving And Underwater Operations," which is published by the Association of Diving Contractors International, Inc. (ADCI)[3]. This standard is often simply referred to as "ADCI."

In this instance, the diver was part of a team using water pumped through an underwater hose to dig a trench in the silty sea floor. This is defined in ADCI, Section 5.35 as "high pressure water blasting." The construction of the trench itself is addressed in Section 5.34, "underwater excavation operations guidelines[3]." With divers working in shifts (in less than 30 feet of water), the trenching operations had been going on for several days at the time of the incident. Units are in U.S. customary units to be consistent with the original work and provided data.

The tool used to dig the trench is a pressure-compensated "jetting nozzle," which receives pressurized water fed by a pump on the barge (as shown in **Figure 2**). The water travels from the pump through a flexible hose through a few swivel fittings to the nozzle. The nozzle is a "tee," where the flow is effectively split into two equal and opposite directions. One end is aimed at the silty bottom to "jet out" the desired trench. The tee is handled so the other end is behind the diver, jetting at the same flow rate as the trenching end — so there is no net force on the assembly. Therefore, there is no force on the diver from the trenching operation.

Figure 3 illustrates the concept of operations prior to the accident. The trench depth reported varied from 36 inches (shown) to 60 inches when completed. The trench section being worked at the time of the incident was reported as being a little past halfway completed. The red oval on the hose shows approximately where the cut is with relation to the diver and equipment. The cut is shown in **Figure 4**.

Figure 2
The jetting nozzle used in the incident. The 90-degree elbow has swivel fittings at both ends. The flow comes from an industrial hose, supplied from the dive boat, and splits at the tee, creating two equal and opposing flows so the jetting force is counterbalanced. The length of flexible hose taped to one end is used to enhance the diver's grip on the forward (or "jetting") end and has no bearing on the flow.

Based on the provided data, the diver was approximately the same dimensions for the 50th Percentile Male as defined by ASTM Standard F1166, "Standard Practice for Human Engineering Design for Marine Systems, Equipment, and Facilities[4]." The previous diver had left the nozzle on the sea bed when he finished his shift and returned to the boat. The incident's diver reported he had followed the jetting hose to the tool, picked it up, and asked the people on the diving boat to turn on the pump. The

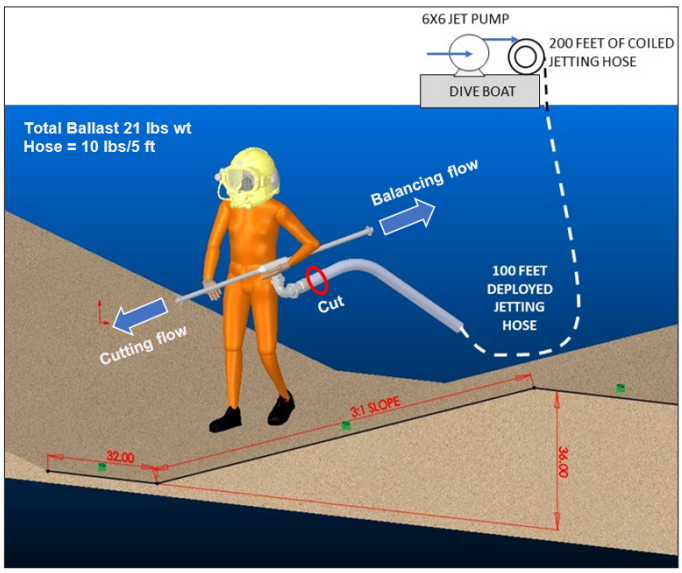

Figure 3
An approximation of the diver typical of a jetting operation. The 3D model is using an ASTM F1166 "50th Percentile Male" in Solidworks Professional. The jetting tool assembly is generally held at the hip and aimed downward in a varying angle to create the trench. The trench dimensions (in inches) are typical for the trenching in this region, and are consistent with ADCI guidance.

Figure 4
Photograph of the end of the jetting hose where it attaches to the coupling. The cut in question is about 9 inches from the coupling once it is screwed into place. In reviewing Figure 3, this places the cut approximately at hip level (location circled in red). The Parker jetting hose is constructed using layers of rubber, plastic, and tire yarn (the same reinforcement used in tires) and is intended to be resistant to cuts and abrasions in an industrial setting.

diver walked along the bottom, maintaining a negative buoyancy by using a diving weight belt. Picking up the hose and jetting nozzle would increase the total weight, acting to hold the diver downward in the soft mud bottom.

The diver picked up the nozzle, held it to his hip, and requested the hose be turned on. He put the nozzle into operation without any issue. This indicated there were no imbalanced forces acting on the nozzle or hose at the time, which, in turn, indicated there was no additional opening in the hose at that time. Suddenly, without any chance to tender on the boat, the diver reported being "thrown around like a rag doll," which included multiple impacts with the silty mud bottom.

The diver reported holding onto the nozzle assembly out of fear and began yelling. The topside crew turned off the jetting pump and was in the process of sending the stand-by diver when the deployed diver reported that was not needed. The diver returned to the boat on his own. The diving team recovered the hose and tool. The diver reported injuries and stated there was some sharp object in the work area that caused the cut in the hose, which, in turn, was the cause for the injuries. The diving team, which was in the dive boat, was not able to observe the work site to confirm the diver's testimony.

The Job Hazard Analysis (per Section 5.9, ADCI)[3] noted this was a natural littoral shallow sea water environment, with associated flora and fauna typical of the region. There had been previous marine operations in the area to include pipe lay for pipelines. Some man-made objects would be expected in these operations. There were no ship wrecks, abandoned structures, or other large hazards known to be in the work site, nor had any sharp objects been reported during previous operations. Other than the cut hose, there is no contention that the previous days of operations failed to conform to ADCI standards or the diving company's safety manual and dive plan.

Chain of Events

The diver had refused medical treatment immediately after the event but later sought medical care for back injuries. The point in contention was whether the back injuries were from the diving incident in question. In order to connect the injury to the incident, a chain of events was developed to specify elements that had to occur in order to establish causality. If the chain of events is proven, then there is direct employment-related causation. It will also justify more detailed work. For example, if the chain of events is not supported, then there is no need to conduct a detailed biomechanical review of the medical files to assess whether the medical documentation is consistent with the physics of the event. If there is no chain of events that connect the employment to the injuries, then the injuries are not due to employment.

The chain of events reviewed is as follows:

- To create the back injuries from the work-related conditions, the diver testified it was due to being repeatedly slammed into the silty seabed.
- To slam the diver multiple times, the diver had to be propelled at impact speeds into the silty sea bed with resulting shock-loading consistent with the reported injuries.
- To be propelled at speeds consistent with injury, sufficient force had to be applied to the diver.
- To develop sufficient force to be consistent with the injury, a corresponding non-compensated mass flow rate was required.
- To create that mass flow rate, a hole in the hose was needed with a corresponding pump-supplied pressure.
- For the diving company to be at fault, the creation of the hole in the hose had to be through no fault of the diver — and in a manner consistent with an argument the diving company failed to provide a workplace free of unacceptable hazards.

Equipment

The pump was a 6×6 jet pump skid using a horizontal split case multi-stage pump. The hose connecting the pump to the jetting tool was a 2.5-inch jet hose. This equipment package can be rented from a number of sources, demonstrating the equipment was typical to the field and could be considered within the normal practice in the field.

The fittings for the nozzle were standard 2.5-inch Schedule 40 90-degree-long radius elbow with swivel fixtures on both ends. One swivel fitting mated to the jetting hose. The other mated to a 2-inch to 1-inch reducing tee. About 24 inches of straight 1-inch Schedule 40 pipe was welded to both ends.

The diver was estimated to weigh 200 pounds. Fourteen pounds of belt weight was necessary to weigh

down the diver enough to work. The total nonbuoyant weight was determined to be 21 pounds, which is the force that had to be countered in order to lift the diver from the bottom. Any change in momentum engages the total mass, but the thrust only has to overcome the nonbuoyant weight to create lift. This neglects the suction force on the feet, which is typical of the environment — a conservative assumption favoring the diver's perspective by assuming "lift off" only has to overcome weight and no resistance due to mud.

The bottom conditions were silty mud into which the divers routinely sank 6 inches to 12 inches. Based on this, it is estimated a torso, with its greater cross-sectional area, would slow over 4 inches before stopping. This was a conservative value as the other divers estimated a person would sink 6 to 8 inches if landing on their back, side, or buttocks based on their kneeling and sitting in that terrain. The hose with water weighed 11 pounds per 60 inches, which means it would take an additional 11 pounds of thrust to lift the diver 5 feet upward before the hose would act as a tether to the ground.

The cut in the hose creates a variable with respect to flow. While the dimensions and location of the cut can be measured, as shown in **Figure 4**, it is unknown whether the cut was extended during the incident. It is also unclear how the various forces on the hose interacted to pull the hole wider. It was noted the location of the cut was relatively close to the coupling. Ergonomically, the operation of the jetting nozzle and carrying the jetting nozzle places this upper section well above the knees of the diver. This is not consistent with the statement that the cut was created by some unspecified man-made object that the company had failed to remove from the area or warn the divers about.

Initial Assessment

The initial question was whether the incident was feasible based on the pump's maximum flow rate. At this phase of the case, details were still being gathered. A "worst-case" method was used to evaluate the potential thrust by water flow based on the jet pump specifications and the hose dimensions.

The length of the hose used and the details of the nozzle were not made available at this point of the inquiry, but the pump specification was provided. The top end of the pump's capacity was 1,400 gal/min, or 5,390 cubic inches per second. If the pump alone, without friction losses and other factors included, could not produce sufficient flow to create significant acceleration, the inquiry could end at that point. Literature associated with evaluating human response to accelerations and impulse (shock) are often presented in term of "G-forces" or multiples of gravity. The calculations and assumptions for this initial assessment are as follows:

Calculate flow for hose without nozzle (assumed 2.5-inch diameter)

$$\boldsymbol{v = (V)/(A)}$$
$$= (5390\ in^3/sec) / (4.91\ in^2) = 1097\ inch/sec$$

Calculate force and impact acceleration (assume fresh water)

$$\mathbf{F\ (thrust) = (V)(\rho)(\mathit{v})/(g_c)} \quad \textbf{[Ref 5]}$$
$$= (5390\ in^3/sec)(0.0361\ lbm/in^3)(1097\ in/sec)/(386\ lbm\text{-}in/lbf\text{-}sec^2)$$
$$= 552\ lb\text{-}f$$

$$\mathbf{F = m*a \rightarrow a\ (thrust) = F(thrust)/m}$$

Taking advantage of U.S. Customary units allows it to be written as in terms of Gs:

$$\mathbf{a\ (thrust) = F(thrust)\ (lb\text{-}f)\ /\ weight\ (lbs)}$$
$$= 552\ (lb\text{-}f)\ /200\ (lbs) = 2.76 \times body\ weight$$
$$= 2.76\ Gs$$

F = force (lb-f)
ρ = density of salt water -= 0.0381 lbs/in^3
v = velocity
m = mass
a = acceleration
V = volumetric flow rate
C_D = drag coefficient
A = cross sectional area with respect to the flow
g_c = gravity constant = 386 lbm-in/lbf-sec^2
G = G-force, or multiples of 386 in/sec^2

Given the maximum thrust acceleration has been determined, use the diver's transcripts and other information to make an initial assessment.

- Assume the calculated acceleration of 2.76 Gs was in effect for 3 seconds before hitting the bottom. The 3 seconds is based on the 30-foot depth, the fact the diver never came close to the surface, and statements by the diver.

- Assume the silty mud bottom stops the diver in 2 inches. This was an initial conservative

assumption that was later revised to 4 inches based on better data.

- As an estimate, use a literature value for a SCUBA diver swimming of $C_D = 0.40$[6]. This is a conservative assumption as the diver in this case was propelled at the waist with a larger cross-section area with respect to the flow rather than a diver propelled forward by his fins. This allows the use of fundamental kinematic relations:

velocity = time * acceleration
(final velocity)^2 = (initial velocity)^2
+ 2(acceleration)(distance)

Given the (final velocity = 0) due to coming to a stop, this can be re-written for calculating the stopping rate as the body contacts the bottom and comes to a stop:

Acceleration$_{(impact)}$ = (velocity at contact)^2 / (stopping distance)

Now applying the previous literature:
speed$_{water}$ = speed$_{air}$/36 [Ref 6]
Velocity = [(3 sec)(2.76 Gs)(386 in/sec)] / 36
= 88.81 in/sec

Acceleration$_{(impact)}$ = (velocity^2)/(2*distance)
= (88.8 in/sec)^2/(2*2 inches)= 1971 in/sec^2
= (a)/386 = 5.1 Gs

Typical literature for correlating accelerations to injury involve ground vehicles or airframes[7-10]. An example of this is shown in **Figure 5**. This generally assumes the person is in some sort of seat with restraints. This incident has no such constraint on the body, which increases the likelihood of injury[9]. An acceleration of 5 Gs is generally below conventional thresholds for injury[7, 9, 10], but 5Gs is consistent with injuries of lateral vehicle impacts[8]. The initial conclusion pump's flow rate does not preclude a diver being injured by being propelled by the maximum flow rate. This initial estimate indicated more detailed analysis was needed.

Verification and Validation

Animations and 3D renderings are treated as an illustration of the expert. Engineering simulations, including computational fluid dynamics, can be seen as a "black box," producing results independent of the expert[11]. This is a potential hazard to the expert witness's testimony. This can be addressed by demonstrating underlying assumptions and data used are appropriate for science-based evidence, "based upon sufficient facts or data," which "are of a type reasonably relied upon by experts in the particular field." The expert also should be prepared to demonstrate the given simulation is "the product of reliable principles and methods" and how the expert "applied principles and methods reliably[12]."

This is also known as "Verification and Validation" (V&V) for simulations. "Verification" is a measure of whether the simulation code can reliably produce accurate and consistent results with sufficient precision. "Validation" is checking the results of simulation by some other means, such as experiments, classical calculations, independently developed simulations, or some combination of techniques. ASME has published V&V20, a guideline specifically for CFD[13].

Solid models of the diver, nozzle assembly and a section of attached hose were developed in Solidworks Professional, a computer-aided design package by Dassault Systemes that also has robust computational fluid dynamic modeling capabilities. Solidworks documents that its CFD package is consistent with the norms for the CFD[14]. Verification is subject to the specific application. CFD is an accepted tool for examining flow through nozzles, including using CFD to validate medical nozzles for the Federal Food and Drug Administration[15], which requires more detail and precision than an industrial jetting nozzle for underwater trenching.

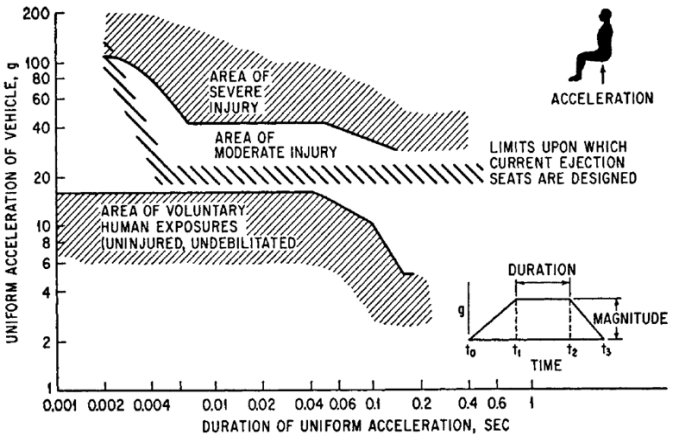

Figure 5
Example of the literature regarding impact acceleration, expressed in "Gs" versus time in terms of injury threshold[10]. This is one of the charts used to assess whether the reported injuries are consistent with the physics. This chart correlated to the diver being driven "butt-first" into the bottom. (U.S. Government report, in public domain)

The resolution of the CFD results was controlled by setting the flow characteristics (mass flow, volumetric flow) to be less than 0.01% of the nominal inputs. The model meshes were refined until the decrease in mesh did not change the results more than 10% from the previous result, consistent with Section 7 of V&V 20[13]. The models were verified by comparing the results to conventional D'Arcy friction flow calculations for the undamaged model as well general agreement with literature, which will be discussed later in this paper.

Developing a More Detailed Analysis

The solid models of nozzle assembly and a section of attached hose are shown in **Figure 6**. The nozzle, fittings, and 60-inch section of hose is one model. The length allows for 10 times the 2.5-inch diameter (25 inches) as an inlet in order to reduce any inlet effects in the model.

A model consistent with the ASTM F1166[4] standard's 50th percentile male figure was developed. The subject was roughly the same height and dimensions as a 50th percentile male, allowing the model to be used without modification other than to have the "clothes" offset 0.25 inches from the body to approximate the wet suit. While the diving hat is shown in **Figure 3**, it is omitted from the CFD models. Omitting the diving hat as well as the weight belt, reserve air tank, and other equipment is a conservative assumption, given the cited study of a SCUBA diver shows a significant increase in drag by adding a larger breathing apparatus, dive knife, and other items less bulky than a diver using surface-supplied air[6]. If the results using the simplified models show the induced drag slows the diver sufficiently to preclude the described events, then a more detailed model with greater drag is not needed.

Additional information was gathered to provide a more detailed analysis. Friction losses in the fittings and hose will decrease pump performance and lower flow rates. Per **Figure 3**, it was determined there was 100 feet of jetting hose deployed and another 200 still aboard the boat. The pump's model and associated performance curve was determined. The fittings and bends of the jet nozzle assembly were tallied up using conventional K-factors to apply the Darcy friction loss method[5].

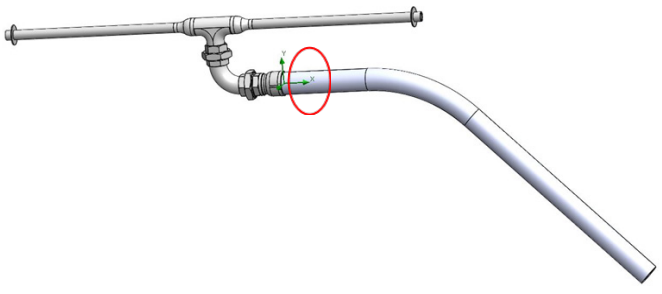

Figure 6
Solid model of the jetting nozzle assembly and 60 inches of jetting hose. This model is used for internal flow of the pressurized water flowing through the nozzle or the nozzle and cut. The red oval shows where the cut is located.

Hoses have different friction factors than pipes. Hoses absorb energy in their side walls, they flex in response to internal as well as external loads, and they vary in construction[16]. Based on the construction of the jetting hose[17], it is assumed the losses can be approximated by the losses associated with a fire hose. The losses for a 2.5-inch fire hose are available in literature[18]. This data allows the fittings to be totaled up and the head loss approximated. The nozzle's symmetrical geometry allows Darcy's equation to be used by adding the two 1-inch pipe flow areas into an equivalent pipe diameter.

$$\textbf{Friction Losses} = (\Sigma K)(v)^2 / (2*g_c) \qquad \textbf{[Ref 5]}$$

K is the friction coefficient factor. For the jetting assembly and hose intact, the total value for K is 18.4, of which 3.6 is what is shown in **Figure 6**: the last bend of the hose, coupling, elbow, tee, and run to sharp exits. The majority of the friction losses are due to flow through the hose.

The effect of the cut in the hose (**Figure 4**) is not well defined. Flow resistance is a function of velocity squared, so as the mass flow into the nozzle is reduced to the cut, the flow rate is reduced along with resistance. The flow through the cut would be the source of thrust while the flow through the nozzle is assumed to remain in balance.

It is possible the hole continued to tear and enlarge during the event. It's also unknown how the forces on the hose shaped the opening. In order to address this, two different sizes of openings are used as well as assuming the hose no longer has a coupling as if all of the flow emptied out through the cut, fully bypassing the nozzle.

The smaller cut is less than the measured cut to address the cut opening further during the incident. The larger cut is larger than the measure opening to address the "yawning" or opening being extended during jetting (**Figure 7**). The smaller effective opening would have a higher velocity, which increases thrust, but a lower mass flow rate, which reduces thrust. The intent is to use a high/low approach that should bracket the effective geometry of

the hole while the hose was pressurized.

The friction losses due to water depth are plotted against the pump curve. Their intersection determines the upstream pressure and flow rate. The losses due to the fittings and opening (or lack of one) changes the effective combined K factor.

A value of 10.8 pounds per 60 inches of jetting hose is used to represent the weight of the hose and water. This is based on the weight per unit length of the hose[17] plus the weight of water within the hose based on wall thickness. This 10.8 pounds per 60 inches (or 0.18 pounds per linear inch of filled hose) is the increased mass the thrust must counter as the diver is lifted away from the bottom. The potential thrust developed is calculated along with the drag and mass currently supported by the thrust. Drag was estimated using conventional drag calculations and the previously cited studies on a swimming diver.

$$\mathbf{F_D = r v^2 C_D A / (2 * g_c)}$$
$$\mathbf{C_D = 2 F_D g_c / r v^2 A} \quad \textbf{[Ref 5, 6]}$$

F_D = drag force, lb-f
r = density in lbm/in^3, which is why g_c is needed
v = velocity
C_D = drag coefficient
A = cross sectional area with respect to the flow (in^2)
g_c = gravity

The first CFD model is the nozzle assembly and hose, shown previously in **Figure 6** and **Figure 7**. The models all had the same outlet conditions for the nozzle as well as the opening in the hose, as applicable. Flow through piping is a classic application of CFD in industry[19]. It is a typical example problem in the mainstream CFD packages, including FLUENT and Solidworks.

The input conditions are based on the flow rate determined by the intersection of pressure losses to the pump curve. The mass flow rate and volumetric flow rate remain linearly proportional for water for the conditions considered. Volumetric flow rate is an input at the open end of the hose, then the analysis reaches equilibrium with the openings, whether it is the nozzle ends, an open end (no nozzle assembly), or the two "cuts" in the hose wall. After the model converged based on output criteria, the model was run again with additional mesh refinement to confirm there was less than a 10% change to the results to ensure the mesh was sufficient. The meshing schemes for the two CFD models are shown in **Figures 8** through **10**.

The regular nozzle model is sufficiently within established literature that the conventional friction loss method should be close to the CFD results. The velocity results of the two are compared to check the CFD assumptions and boundary conditions. If the two are within 10%, the CFD model has converged on a flow rate that agrees with the conventional methods. It is expected the CFD will have a higher velocity due to the CFD model including laminar boundary layers, or "wall effects," which act to constrict the flow channel, whereas the conventional method neglects these details and assumes flow is uniform through the full cross-sectional area. If these two methods are in sufficient agreement, there is sufficient confidence in the other models. The open hose (no nozzle assembly) was calculated as a worst-case condition (maximum thrust), given the nozzle assembly remained on the jetting hose.

The other model was an external flow of water

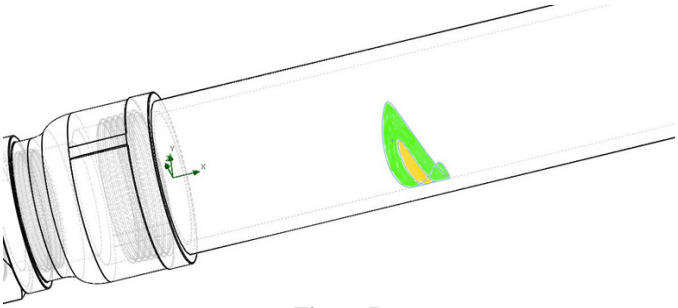

Figure 7
Detailed view of the model of the hose as it transitions into the coupling. The interior of the hose is inscribed with split-lines that can be set as outlets in CFD. The yellow shows the smaller opening with 0.375 square inches. This represents a possible small initial cut. The green shows the outline of the larger hole, which represents the length of the cut. The two colored regions total 2.00 square inches.

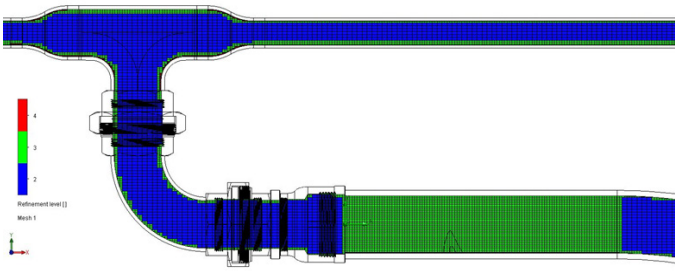

Figure 8
A 2-D projection of the 3-D mesh for the CFD model of the nozzle assembly and hose section. The blue regions represent the nominal mesh. Green areas are subdivided by one step, quadrupling the mesh density. Red is yet another subdivision. Typically, these subdivisions are used to locally refine the mesh to address changes in geometry, such as corners or channels. This is seen along the outside edges of the assembly. The region of the hose around the cut has been assigned a subdomain to control the mesh locally in a uniform manner, as illustrated with the large section of green.

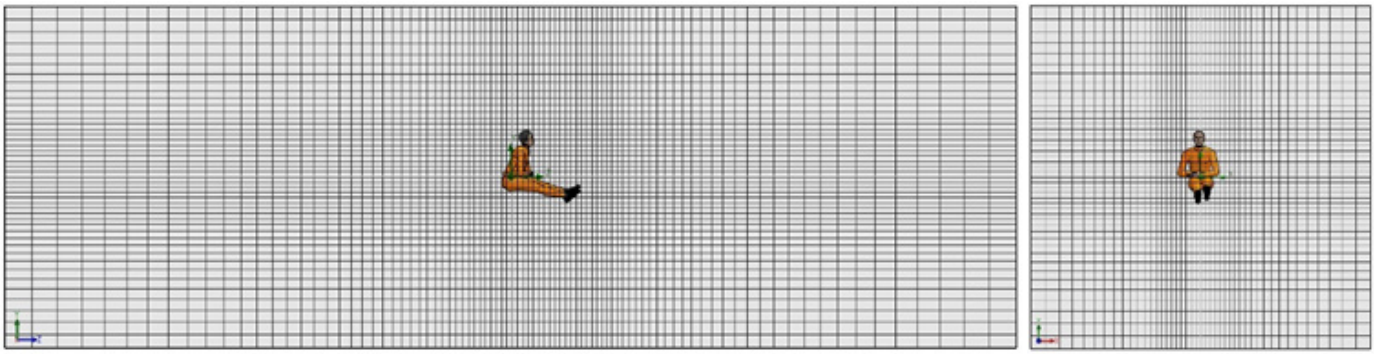

Figure 9

Macro mesh of the external flow around the diver. CFD meshes allow for larger aspect ratios than other computational applications such as Finite Element Analysis. The mesh is more refined and square around the model of the diver. A uniform, fully turbulent flow is assumed with a macro velocity of 20, 60, 100, 200, and 300 inches/second. The cross-sectional area of the diver with respect to the flow is about 530 square inches.

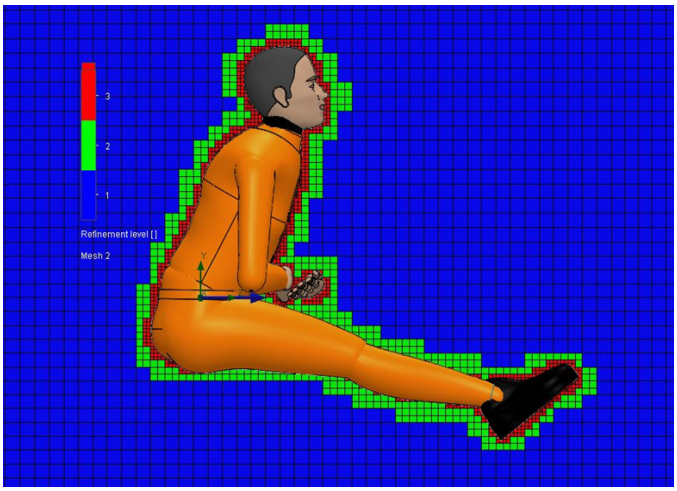

Figure 10

Detailed view of the mesh projected along the centerline of the computational domain. The 3D figure is also centered along the centerline. Diving hat, reserve air, umbilicals, and other equipment are omitted, which significantly reduces drag[6]. Similar to Figure 7, the color code shows the amount of mesh refinement, which is part of the Verification and Validation (V&V) process.

flowing around the diver as if being propelled backward. This is similar to other applications, such as CFD analysis of torpedoes[20,21]. Modeling the flow on the object returns the reaction force. The reaction force, in turn, is the force needed to propel the object at that speed. With a torpedo, it indicates the thrust the motor needs to produce. In this scenario, it's the thrust generated by the mass flow through the hole in the hose. The selected flow rates were 20, 60, 100, 200, and 300 inches/second. The upper limit is about 17 mph, which is consistent with a low-speed impact by a vehicle that is likely to cause injury. The other values are progressively less.

It is recognized that the diver did not maintain a rigid body posture during the reported event. The intent is to approximate the force needed to propel a body through the water in the manner described. It would also serve as a visual exemplar of the fluid dynamics in play — something that is challenging to communicate to a lay audience.

The nature of the hose cut is one of the primary issues related to liability. The hose was sent to an independent laboratory for measurements and an additional professional opinion regarding the characterization of the cut shown in **Figure 4**. The nature and origin of the cut was addressed as part of the overall forensic engineering analysis, but is not central to the topic of this paper.

Results

The bulk of the friction losses occur prior to the cut. The Darcy Friction Loss method is well suited for well-defined geometry, such as the majority of the hose, but it is not well suited for the irregular geometry of a cut in the side of a hose. Assuming the conditions before the cut provides the baseline flow rate, shown in **Figure 11** and **12**, the effects of the cut are shown in **Figures 13** through **16**.

The results are summarized in **Figure 17**. The significance is as follows:

- The "no cut" CFD model is consistent with the Darcy friction loss results, which validates the models.
- The force of the nozzle (F nozzle) is provided as part of the checks but does not contribute to the motion of the diver as the listed force is two such forces in opposite directions.
- The flow rate increased with more outlets or larger outlets but not by more than a few percent. This is

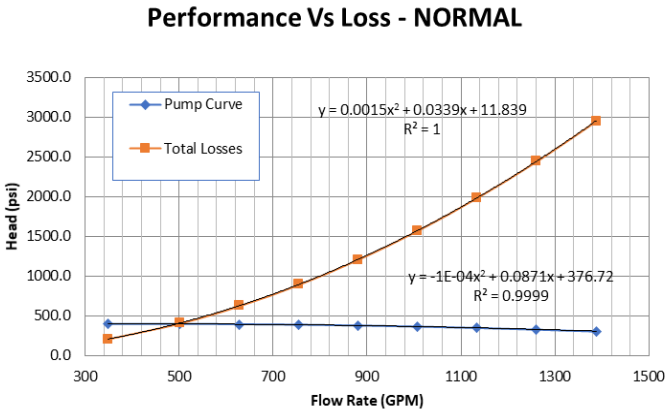

Figure 11

The friction losses and pump curve for the tee installed and no cut in the hose intersects at 494 gpm, or 1903 cubic inches/second. The small changes in total losses ("K") creates a minor change in each model's "total losses." The two equations from curve fitting are solved to determine the volumetric flow rate in GPM.

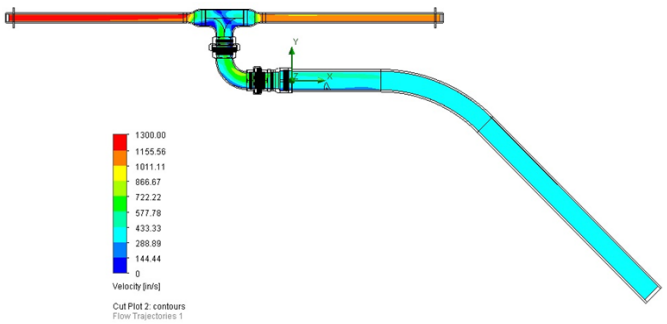

Figure 12

CFD velocity plot of the nozzle assembly and hose section plotted along the centerline. It illustrates how flow velocity increases as the pipe reduces in area. This is the baseline for velocity. While there is a slight bias of higher velocity to the left branch, the forces generated at each exit are approximately equal.

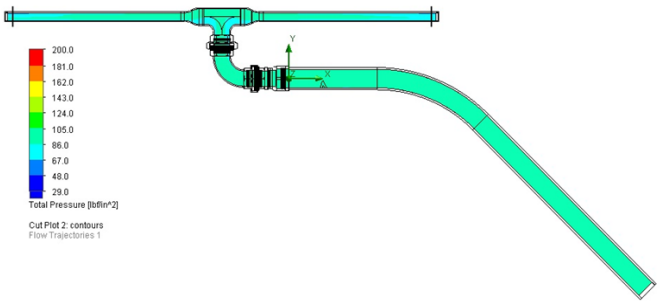

Figure 13

CFD pressure plot for large cut model plotted along the centerline. There is not a great pressure deviation over this relatively small model. This confirms the pressures indicated using friction loss methods.

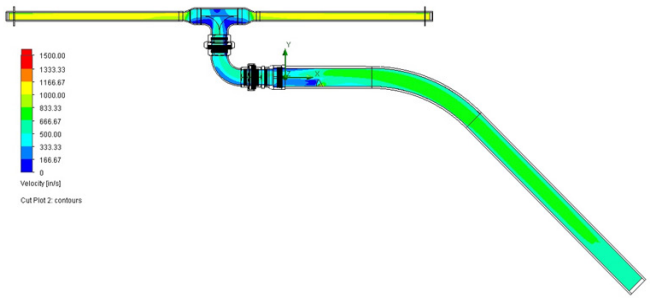

Figure 14

CFD velocity plot of the large cut model plotted along the centerline. This shows a significantly different trend from Figure 12. More detailed views will follow.

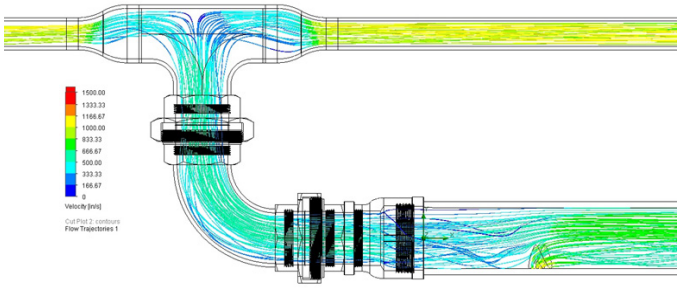

Figure 15

CFD velocity plot using particle tracing of the large cut model. This is one of the visualization methods that makes CFD a useful tool to illustrate complex flow conditions. The flow lines started on the hose inlet with 40 equally spaced start points, which followed the flow line from that position. This illustrates how flow pushes into the tee, then splits into two paths. The colors in this case correspond to velocity, but the same flow lines could be plotted with pressure, temperature, viscosity, and other properties. Other options are iso-contours, such as a curved plane of all the same pressure or velocity, as well as plotting on the surface of models or using multiple flat planes. The region highlighted with the dashed lines is the region of the cut and is shown in more detail in the next figure.

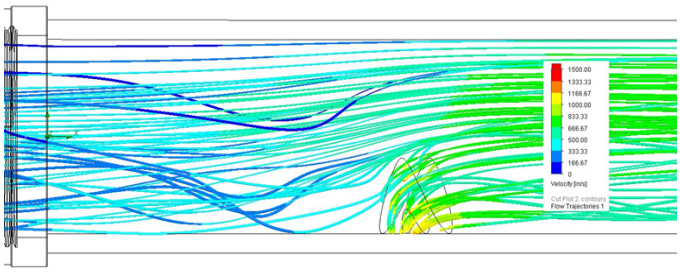

Figure 16

CFD velocity plot using particle tracing of the large cut model showing a detail of the cut area. This shows many of the flow lines terminating in the cut, illustrating how a portion of the flow is diverting out of the cut but the rest flows around the cut. It also illustrates how the flow is accelerating at the cut but has a velocity is reduced immediately downstream of the cut.

Summary of Results										
Condition	Flow (GPM)	K total	Vnoz	Mass flow rate (lbm/sec)			F Nozzle (lbf)	F Open (lbf)	Net Thrust (lbf)	Initial Gs
				Total	Nozzle	Opening				
No Cut (Darcy)	494.4	18.4	1057.5	72.5	72.5	n/a	94.0	n/a	n/a	n/a
No Cut (CFD)	494.4	18.4	1120.0	72.5	72.5	n/a	105.4	n/a	n/a	n/a
Small (CFD)	505.0	17.5	830.0	74.1	64.8	9.3	57.9	19.8	none	none
Large (CFD)	511.3	15.9	609.7	75.0	23.4	33.6	31.2	51.6	30.6	0.2

Figure 17
While the plots help illustrate complex flow, the detailed numerical results are often done by selecting model faces and querying the conditions at that location. This table represents a summary of key results.

consistent with the fact the majority of the losses are due to the friction losses prior to reaching the cut and nozzle assembly, so the variations in this model are not driving the flow conditions.

- The small cut's force is less than the 21 pounds of ballast, so it is insufficient to lift the diver. While it could push the diver sideways, it would not conform to the statements of "being picked up and slammed down repeatedly."

- The G forces are calculated using the net total force applied to the total mass of the diver. The G forces indicate the statements of "being picked up and slammed down repeatedly" is not consistent with the physical limitations of the system.

The drag was determined by using the program to sum the forces on the diver's model and breaking it out into the x, y, and z directions. The drag forces are the z-direction. The values for C_D are determined by using Eqn. 4 and the projected area of 530 square inches of the diver with respect to the flow. The G forces are calculated assuming the baseline speed (Z velocity) is achieved, and then the diver impacts into the muddy bottom, stopping in 4 inches.

The drag coefficient is somewhere between the literature value for a sphere (0.47) and a cone (0.52), which appears to be consistent with the torso being generally perpendicular to the flow and the legs trailing. By comparison, a streamlined body has a C_D of 0.04 to 0.09. Comparing it to literature, the value for C_D of a diver in a prone, head-first attitude to the flow is between 0.38 and 0.42[6]. Since the results of the upright diver (without equipment) has a higher value for C_D than the literature for a prone diver, the results for this study are generally consistent with the physics regarding flow and drag. Drag is fairly simple to visualize on simple bodies like a cube or sphere, but explaining how drag works on a complex shape is more challenging. **Figure 18** and **Figure 19** show how some of these complex flows can be visualized, including how the drag builds up as a pressure resistance.

The significance of the table shown in **Figure 20** is the force on the diver at a given flow rate. This, in turn, would be the jetting force needed to propel the diver at that speed. The maximum rate of 300 inches/second (about 17 mph) corresponds to a speed consistent with a person being struck in a low-speed vehicle impact[7-10]. This would require 1,123 pounds of thrust. The resultant G-forces in **Figure 20** are based on assuming 4 inches of stopping distance.

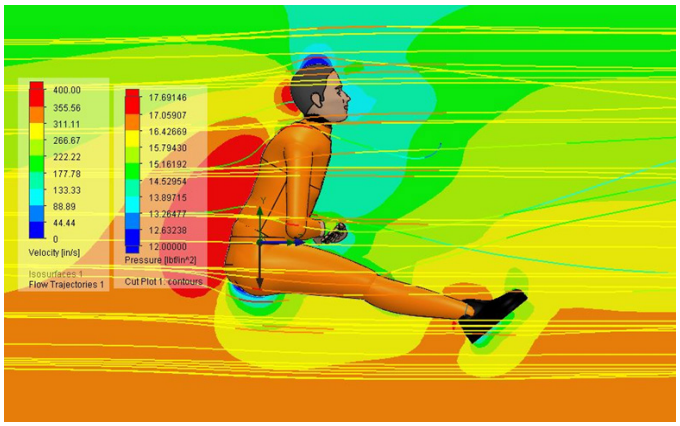

Figure 18
CFD plot of diver in a 300 inches/second flow. This is the maximum rate analyzed. While the simulation is holding the person stationary and producing a flow from left to right, this would produce the same reaction forces and flow effects of the diver being propelled from right to left in still water. This is a more complex plot to illustrate more of the potential for producing exemplars and technical illustrations. The centerline plot is a pressure plot, illustrating a higher pressure region on the diver's back and a low pressure area consistent with lift on the head. The streaks are a particle plot showing the velocity with yellow being the baseline velocity and other colors showing increases or decreases. This could be used to explain the relationship of higher velocity to lower pressure to a specific situation to a lay audience.

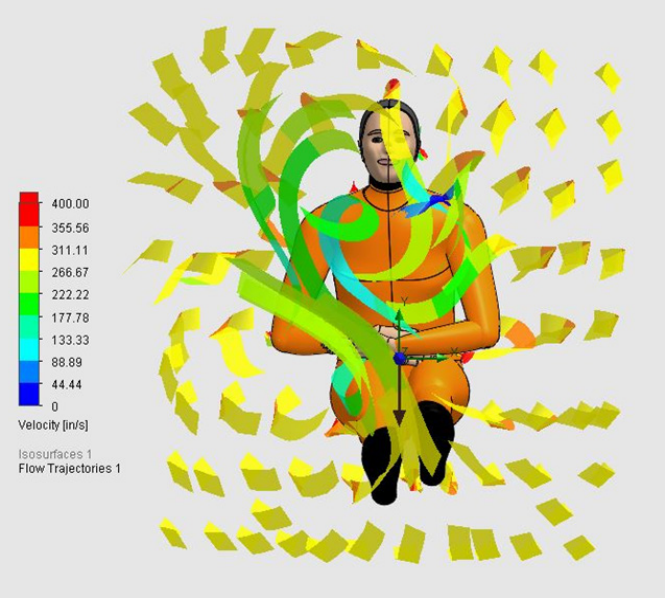

Figure 19

CFD particle plot of the diver in 300 inches/second flow. This particle plot using "ribbons" instead of "lines." The ribbons provide more visual discrimination. This is used to show the swirling around the diver as the flow goes past. One use would of this could be to illustrate how being propelled in this manner would further disturb the silty bottom and obscure the diver's vision as well as anyone observing.

The speed values neglect the time and distance needed to accelerate to maximum speed as well as neglecting the increasing weight due to lifting the jetting hose filled with water. The increasing weight would counter the thrust and slow the diver's speed. Once the total thrust equaled the total weight suspended by the jet, the jetting hose would act as a tether, constraining motion within that length.

Indexing the net thrust from (**Figure 17**) to the force needed to sustain the speeds in (**Figure 20**):

Small Cut: Cannot lift due to the force is less than the 22 pounds net ballast at start.

Large Cut: Net thrust is 30.6 lbf
Speed between 20 in/sec and 60 in/sec
Estimate impact less than 1.2 Gs
Max. distance = 13.9 ft with increasing loss of net thrust due to hose weight

The estimated impact is using very conservative values that favor the diver's perspective. Adding a tank significantly increases the drag[6], let alone the rest of the diving equipment that was not modeled. This summary was presented to appropriate medical professionals in order to assess whether the injuries are consistent with the physics after the report was submitted.

3D CFD on Diver Body			
Z vel (in/s)	*F(drag) (lbf)*	*C(drag)*	*G's @4in*
20	5.5	0.526	0.1
60	45.8	0.486	1.2
100	128	0.489	3.2
200	513	0.490	13.0
300	1123	0.477	29.1

Figure 20

This shows the result of five CFD runs of different flow speeds. The drag the diver experiences being stationary to the z-direction flow is the same force needed to propel the diver at that speed through still water. In order to propel the diver 300 inches/second (about 17 mph) as depicted, the water jet would have to produce 1,123 lb-f of thrust. This table is used to assess the diver's potential speed based on the results for the force due to mass flow through the hole in the hose.

Separate from the CFD studies, a third-party independent laboratory concluded the cutting of the reinforced wall of the Parker jetting hose was done by a sharp tool in a deliberate sawing motion and was not consistent ergonomically or mechanically with the hose contacting something sharp on the bottom of the trenching area. Its proximity to the jetting tool was assessed by the author and the laboratory to be consistent with a person holding the tool for leverage and using a utility knife, such as those commonly worn by commercial divers. The diver in question had a diving utility knife with a serrated blade consistent with the tool marks on the jetting hose.

Conclusions

- There is no evidence to support the diving company failed to maintain a safe work area in a manner consistent with the work required, profession, and training of the people.
- The location of the cut and third-party laboratory reports indicate the hose cut was consistent with a deliberate sawing action while being held and was not consistent with being dragged along the ground and cut by an unidentified object.
- The propulsive force of the pumped water would be limited by the weight of the jetting hose and water, reducing acceleration significantly the more the diver lifted or was pushed around the bottom.
- The pumped water exiting the cut in the house could not provide sufficient water flow to propel the diver in the manner described, both in terms of lifting the person violently as well as forcing violent contact with the bottom.

- The velocities calculated using the simplified conservative models are not consistent with the literature values associated with injury. Final determination of the relationship of available velocity and acceleration to the injuries was done by an appropriate medical professional qualified in evaluating these types of injuries.

- In summary, the diver's report of the underwater events is not consistent with the physics associated with the equipment in use in the reported configuration and operating conditions.

References

1. L. L. Liptai, "Forensic Engineering And The Scientific Method," Journal of the National Academy of Forensic Engineers, vol. 26, no. 1, 01/01 2009, doi: 10.51501/jotnafe.v26i1.711.

2. OSHA Laws & Regulations, O. S. H. Administration 29 CFR 1910 Subpart T "Commercial Diving", 2011.

3. International Consensus Standards For Commercial Diving And Underwater Operations, ADCI, Houston, Texas, 2011. [Online]. Available: https://www.adc-int.org/content.asp?contentid=173.

4. F1166-07 Standard Practice for Human Engineering Design for Marine Systems, Equipment, and Facilities, ASTM, West Conshohocken, PA, 2013. [Online]. Available: https://www.astm.org/Standards/F1166.htm.

5. *Flow of fluids through valves, fittings and pipe:* Technical Paper 410. Stamford, CT: Crane Valves, 2011.

6. M. A. Passmore and G. Rickers, "Drag levels and energy requirements on a SCUBA diver," Sports Engineering, vol. 5, no. 4, pp. 173-182, 2002, doi: 10.1046/j.1460-2687.2002.00107.x.

7. C. Harris and A. G. Piersol, *Harris' Shock and Vibration Handbook*, 2009, New York, NY: McGraw-Hill, 6th ed., 2009, p. 1168.

8. M. M. Panjabi, P. C. Ivancic, Y. Tominaga, and J.-L. Wang, "Intervertebral Neck Injury Criterion for Prediction of Multiplanar Cervical Spine Injury Due to Side Impacts," Traffic Injury Prevention, vol. 6, no. 4, pp. 387-397, 2005/12/01 2005, doi: 10.1080/15389580500257100.

9. "Test methodology for protection of vehicle occupants against anti-vehicular landmine effects : final report of HFM-090 Task Group 25," in "RTO technical report," NATO Research & Technology Organisation;, Neuilly-sur-Seine, 9789283700685, 2007, vol. 90. [Online]. Available: https://www.tib.eu/de/suchen/id/TIBKAT%3A578708116.

10. A. M. Eiband, "Human tolerance to rapidly applied accelerations: a summary of the literature," NASA, June 1959. [Online]. Available: https://ntrs.nasa.gov/citations/19980228043.

11. C. D. Walker. "Using Computer-Generated Animation and Simulation Evidence at Trial: What You Should Know." American Bar Assocation. https://www.americanbar.org/groups/litigation/committees/products-liability/practice/2018/using-computer-generated-animation-simulation-evidence-at-trial/ (accessed October 17, 2019).

12. V. Webster and F. Bourn, "The Use of Computer-Generated Animations and Simulations at Trial," Defense Counsel Journal, vol. 83, pp. 439-459, 10/01 2016, doi: 10.12690/0895-0016-83.4.439.

13. V&V 20 Guide For Verification And Validation In Computational Fluid Dynaics and Heat Transfer, ISBN 9780791873168, ANSI/ASME, New York, 2009.

14. A. V. Ivanov, T. V. Trebunskikh, and V. V. Platonovich. "Validation Methodology for Modern CAD-Embedded CFD Code." Dassault Systemes. https://www.solidworks.com/sw/docs/Flow_Validation_Methodology-Whitepaper.pdf (accessed 18 December, 2019).

15. P. Hariharan, G. A. D'Souza, M. Horner, T. M. Morrison, R. A. Malinauskas, and M. R. Myers, "Use of the FDA nozzle model to illustrate validation techniques in computational fluid dynamics (CFD) simulations," PLOS ONE, vol. 12, no. 6, p. e0178749, 2017, doi: 10.1371/journal.pone.0178749.

16. Neutrium. "Pressure Losses in Hoses." https://neutrium.net/fluid_flow/pressure-loss-in-hoses/

(accessed 12 Sept., 2017).

17. "Series SS122 Lightweight Water Jetting Hose." Parker Hoses. https://ph.parker.com/us/15551/en/lightweight-water-jetting-hose (accessed 12 Sept., 2017).

18. Firedepartment.net. "2.5" Fire Hose Friction Loss Calculator." https://www.firedepartment.net/fire-dept-tools/printable-friction-loss-calculator/two-and-a-half-inch (accessed 21 Sept., 2017).

19. A. Pasha, A. Mushtaq, and K. Juhany, "Numerical Study of Heat Transfer of Water Flow through Pipe with Property Variations," Athens Journal of Technology and Engineering, vol. 4, pp. 359-385, 12/01 2017, doi: 10.30958/ajte.4-4-4.

20. J. V. N. Sousa, A. R. L. Macêdo, W. Amorim Jr, and A. G. B. Lima, "Numerical Analysis of Turbulent Fluid Flow and Drag Coefficient for Optimizing the AUV Hull Design," Open Journal of Fluid Dynamics, vol. 4, pp. 263-277, 09/01 2014, doi: 10.4236/ojfd.2014.43020.

21. G. M. Wilcox, "Drag Studies in Water Entry of the MK 13-6 Torpedo," California Institute of Technology, Pasadena, CA, July 1951 1951. [Online]. Available: https://authors.library.caltech.edu/57351/1/E-12.1.pdf.